THE IRAQI JOURNAL OF
VETERINARY MEDICINE
eISSN:2410-7409
pISSN: 1609-5693

OPEN ACCESS

Characterization and Animal Skin Irritations Investigation of Vemurafenib Microemulsion-Based Hydrogel Using Oily Ionic Liquid

Mohammed J Neamah , Entidhar J Al-Akkam*

Department of Pharmaceutics, College of Pharmacy, University of Baghdad, Baghdad, Iraq

***Correspondence**:
drentidhar@copharm.uobaghdad.edu.iq
Received: 26 June 2023
Revised: 08 August 2023
Accepted: 03 September 2023
Published: 28 June 2024

DOI:
https://doi.org/10.30539/8z83dp63

Cite:
Neamah MJ, Al-Akkam EJ. Characterization and animal skin irritations investigation of vemurafenib microemulsion-based hydrogel using oily ionic liquid. Iraqi J. Vet. Med. 2024;48(1):81-92.

A B S T R A C T

Cutaneous melanoma accounts for a yearly mortality rate of 55,500 persons. The use of oral small-molecule kinase inhibitors, specifically targeting BRAFv600, has been licensed as the principal treatment strategy for managing both locally progressed and metastatic presentations of the condition. Approximately 30% of people on vemurafenib, a BRAFv600 inhibitor, have side effects when are taken orally. Objective: This research was attempted to develop a vemurafenib microemulsion by substituting conventional oil phases with ionic liquids (ILs). The microemulsions were created by dissolving vemurafenib in a combination of ionic liquid (1-Butyl-3-methylimidazolium hexafluorophosphate and 1-Octyl-3-methylimidazolium hexafluorophosphate) and surfactant (Triton x-100). Multiple tests were conducted to measure physical stability, pH determination, content homogeneity examination, and in vitro medicine release analysis. Four formulations of Vemurafenib microemulsions successfully met all criteria in the microemulsion characterisation and assessment tests. The droplet sizes in these microemulsions fell inside the range of microemulsions, which is less than 200 nm. They were then used to create microemulsion-based hydrogels, employing Carbamer 340 as a gelling agent by conducting a simple mixing method. Hydrogels formed from microemulsions containing 1-Octyl-3-methylimidazolium hexafluorophosphate demonstrated the ability to form clear hydrogels with desirable consistency. Regarding Ex-vivo permeability study and skin deposition the permeability profiles of GOT3 formula exhibits a permeability measurement of 33569± 344 mP.s at 6 rpm, whereas GOT4 demonstrates a permeability measurement of 54723± 380 mP.s at 6 rpm. During the skin irritation test, there was no apparent erythema and edema were observed when compared to the negative group. This may indicate that the designed microemulsion-based gel formulation demonstrates good biocompatibility with skin tissue. Topical delivery of vemurafenib is a promising route of drug administration to melanoma skin. Ionic liquids (ILs) have permeation-enhancing properties with either hydrophilic or lipophilic characteristics.

Keywords: vemuraenib, microemulsion, ionic liquid, pseudoternary phase diagram

INTRODUCTION

Cutaneous melanoma accounts for a yearly mortality rate of 55,500 persons. The global incidence and mortality rates of this illness showed substantial disparities, principally affected by variables such as the availability of early detection modalities and the accessibility of primary healthcare facilities (1). The management of locally progressed and metastatic forms of melanoma, the BRAFv600-mutated subtype that affects 50% of patients, has been licensed to be primarily treated with oral small-molecule kinase inhibitors identified as

BRAFv600 inhibitors. Vemurafenib is a pharmaceutical compound that acts as an inhibitor specifically targeting the oncogenic BRAF kinase (2).

It has demonstrated substantial improvements in progression-free and general survival, in addition to high quantitative response rates, which established it as a groundbreaking model of a BRAF inhibitor (3). Around 30% of patients who orally administered vemurafenib experience unpleasant effects, potentially necessitating the cessation of treatment (4). Furthermore, it is important to note that the stability and instability of crystalline phases of vemurafenib have limited solubility in aqueous solutions, as evidenced by a concentration of less than 0.1 µg/mL (3).

Systemic administration of vemurafenib is associated with a heightened probability of experiencing side effects. As a result, efforts have been concentrated on developing a localized formulation of this therapeutic compound in order to assist patients carrying the BRAFV600E kinase mutation in the treatment of melanoma (5). Microemulsions are a kind of colloidal system that consists of small liquid droplets scattered throughout another liquid medium. These droplets have the potential to dissolve both lipophilic (fat-soluble) and hydrophilic (water-soluble) medicines. Additionally, microemulsions exhibit long-lasting thermodynamic stability. Microemulsions have been discovered to effectively enhance the cutaneous and transdermal administration of medicinal substances due to their capacity to assist the transportation of high molecular weight medicines into the skin (6, 7).

Microemulsion exhibits a wide range of microstructural configurations, including reverse micelles that consist of water-in-oil (w/o) droplets, expanded oil-in-water (o/w) micelles, and non-uniform bicontinuous microstructures with minimum to no mean curvature. Microemulsion is often used as a vehicle for administering lipophilic medications, while water-in-oil emulsion is typically utilized for delivering hydrophilic pharmaceuticals (8). The organic solvents that make up the oil phase of microemulsions (MEs) often exhibit volatility, toxicity, and flammability characteristics. These particular attributes are deemed to have negative consequences for their environmental implications (9).

Malignant melanoma ranks as the prevailing neoplasm in the oral cavity of dogs, often leading to a poor prognosis. This is attributed to its aggressive local manifestation, high tendency for metastasis, and resistance to conventional treatment approaches. Melanocytic-origin tumors constitute the primary intraocular neoplasms in cats, among which feline diffuse iris melanoma is the most prevalent. Early removal is crucial for a favorable prognosis, as delayed intervention poses risks of systemic metastasis (10).

An ideal animal model should precisely replicate human illness, specifically focusing on the molecular genetics and histological structure of cutaneous melanoma. Moreover, it should be capable of being altered by genetic and immunologic methods. Several animal melanoma models have been discussed, although the histological characteristics and course of melanocytic malignancies in animals are largely different from those in human cutaneous melanoma. Previous studies have identified large animal models of melanoma such as Sinclair swine and Camargue horse, however none of them develop melanomas due to exposure to sunshine. The Xiphophorus fish model, which is non-mammalian, has been used for research on the photobiology and genetics of melanoma. The Xiphophorus fish naturally forms melanomas and is sensitive to UV radiation, although the characteristics of the tumors are significantly different from human melanomas (11).

Mice are an excellent animal model primarily because of the comprehensive knowledge of mouse genetics, yet initiating melanomas in mice is quite challenging. Additionally, melanomas that develop in animal models usually originate in the dermis and do not have histopathologic resemblances to human diseases. Mammalian melanomas presumably originate from the skin due to the typical positioning of melanocytes inside the skin (12).

The objective of this research was to develop a vemurafenib microemulsion by substituting conventional oil phases with ionic liquids (ILs).

MATERIALS AND METHODS

Ethical Approval

The research was approved by the Protocol Review Committee at the College of Pharmacy at the University of Baghdad, with the reference number REACUBCP33023A. The study adhered to the standards for the Care and Use of Laboratory Animals as outlined in the publication No. 85-23, amended in 1996, by the US National Institutes of Health (NIH).

Chemicals

The materials utilized in this study included the Vemurafenib (Hangzhou Hyper chemicals, China), 1-Butyl-3-methylimidazolium hexafluorophosphate and 1-Octyl-3-methylimidazolium hexafluorophosphate (Hangzhou Hyper chemicals, China), Triton X-100 (TX-100, HiMedia, India), hydroxypropylmethyl cellulose (HPMC K 15 M) (hyper chem, China), Carbomer 340 (Tinci, China), potassium dihydrogen phosphate (KH_2PO_4), disodium hydrogen phosphate (Na_2HPO_4), and hexadecyltriammonium bromide (HTAB, HiMedia, India).

Constructing Ternary Phase Diagram

The study conducted a phase behavior analysis to identify the microemulsion region and develop a predictive model for determining the appropriate amounts of the surfactant (TX-100), oil phase (represented by ILs such as

1-Butyl-3-methylimidazolium hexafluorophosphate or 1-Octyl-3-methylimidazolium hexafluorophosphate), and water required to form a stable microemulsion. The procedure used for the study consisted of mixing ILs with TX-100 in different weight ratios, encompassing 1:9, 2:8, 3:7, 4:6, 5:5, 6:4, 7:3, 8:2, and 9:1 (ILs: TX-100 w/w). Following that, water was gradually added to each combination with mild agitation until the point of turbidity was attained. The precise measurements of water (in grams) given to each oil: surfactant mixture was carefully documented, and the weight percentages of the individual ingredients, namely oil, surfactant, and water, were calculated and organized for the construction of a ternary phase diagram (13, 14).

Preparation of Microemulsions

Microemulsions (MEs) were prepared by dissolving 10 mg of vemurafenib in various combinations of ILs and surfactants, followed by vigorous agitation until the medication was completely solubilized in the oil phase. A surfactant combination was obtained. Afterward, an appropriate amount of water was slowly added in small increments over 10 minutes, resulting in formation of a uniformly transparent mixture. The produced formulations were thereafter allowed to equilibrate for 24 h (15). A total of six microemulsion formulations were produced. The formulas denoted as BT1-BT3 were synthesized using 1-Butyl-3-methylimidazolium hexafluorophosphate (BMIM) as the oil phase. Formula BT1 consists of 10% w/w BMIM, 60% w/w TX-100, and 30% w/w water. The composition of Formula BT2 consists of 10% w/w BMIM, 70% w/w TX-100, and 20% w/w water. Formula BT3 consists of 15% w/w BMIM, 60% w/w TX-100, and 25% w/w water. The formulas denoted as OT1-OT3 were synthesized using 1-Octyl-3-methylimidazolium hexafluorophosphate (OMIM) as the designated oil phase. Formula OT1 consists of 10% w/w OMIM, 60% w/w TX-100, and 30% w/w water. The formulation denoted as OT2 consists of 10% weight/weight (w/w) octyltrimethylammonium methyl sulfate (OMIM), 70% w/w Triton X-100 (TX-100), and 20% w/w water. The composition of Formula OT3 consists of 15% w/w OMIM, 60% w/w TX-100, and 25% w/w water, as shown in Table 1.

Table 1. Constituent configuration of various vemurafenib microemulsions

Formula No.	Vemurafenib % w/w	ILs % w/w	TX-100 % w/w	Water % w/w
BT1	0.2	10	60	30
BT2	0.2	10	70	20
BT3	0.2	15	60	25
OT1	0.2	10	60	30
OT2	0.2	10	70	20
OT3	0.2	15	60	25

Characterization of MEs

Percentage transmittance and refractive index

In order to determine the relative transmittance of the MEs formulas (BT1-BT3 and OT1-OT3), their transparency was evaluated using a UV–visible spectrophotometer (UV-1900I PC Shimadzu, Kyoto, Japan). MEs study was carried out at a reference wavelength of 650 nm, utilizing distilled water as the negative solution. The mean values were documented after the completion of three repetitions (16, 17).

Measurement of particle size, polydispersity index and zeta potential

The Zestasizer instrument (Malvern, UK) was utilized to determine the BT1-OT3 and BT1-BT3 formulations' particle size and polydispersity index (PDI). A volume of 1 mL was obtained from every specimen and afterward diluted with deionized distilled water to a final volume of 3 mL (18). After that, the attenuated formulations were introduced into the apparatus, which allowed for the evaluation of each formulation's particle size and PDI (19)

Dilution test

To ascertain the composition of the produced microemulsions, specifically whether they were water-in-oil (w/o) or oil-in-water (o/w), a dilution test was conducted. The evaluation process involved adding 1 mL of each manufactured formulation to deionized distilled water, followed by a visual inspection of the formulations for absence of turbidity and optical clarity (20).

Electrical conductivity test

Conductivity measurements play a crucial role in offering valuable insights into the properties of the resultant microemulsion system, particularly in distinguishing between w/o and o/w MEs. The quantification of electrical conductivity (σ) was employed to assess the extent to which the chosen viscous mixture dissolved the water phase. A conductivity meter was utilized to determine the electrical conductivity (σ) of the formed samples (TDS Ec Meter Temperature Tester, China) (21).

Physical stability tests

The evaluation of MEs' physical stability was conducted utilizing a dual methodology. The initial assessment comprised a heating-cooling cycle experiment wherein the synthesized MEs were exposed to specific temperatures (4, 25, and 40 °C) for a minimum of forty-eight at each temperature. The produced MEs were then subjected to storage conditions at -20 °C and 25 °C for a total of 48 h as part of the subsequent evaluation, referred to as the freeze-thaw cycle test. The freeze-thaw cycle was repeated three times. After every cycle, the MEs underwent a

comprehensive analysis in order to identify any indications of phase separation or turbidity, as established in prior research (22, 23).

pH measurement

The pH measurement was conducted using a pH meter instrument (HANNA RI 02895, Romania). The process of calibrating the instrument included the use of standard buffer solutions with pH values of 7 and 4. Following the calibration process, the probe of the device was submerged into each of the created microemulsions, namely the BT1-BT3 and OT1-OT3 formulations. Subsequently, the pH values obtained from these immersions were properly registered (24).

Drug content test

The evaluation of drug content was conducted by diluting each designed microemulsion (100 mg of ME) with methanol to an appropriate concentration for spectrophotometric analysis (10 mL). The concentration was determined by measuring the absorbance at the wavelength of maximum absorbance (λmax) at 305 nm (25). The drug content of each formulation was assessed by comparing the measured content with the theoretical drug content, which was computed using the equation provided below (25).

$$\text{Drug content (\%)} = \frac{\text{Actual drug content}}{\text{Theoretical drug content}} \times 100$$

In-vitro Drug Release

The dialysis bag approach was used to perform *in-vitro* drug release analyses. Dialysis bags with pore diameters ranging from 8000 to 12000 Dalton were employed for this purpose. The dissolving media used in this study was the dissolution medium recommended by the FDA for vemurafenib. A 0.1 concentration of HTAB was added to a 0.05 M phosphate buffer solution with a 6.8 pH. The examination commenced with the dialysis bag being submerged in the designated dissolving liquid for a period of 24 h to saturate it. Subsequently, a gram of each formulation was transferred into the hydrated dialysis container, which was then sealed on all sides. The concentrated solution contained in the dialysis container was introduced into a 100 ml volume of dissolving medium. The system was subsequently rotated at a rate of 50 rpm, with a temperature regulation of 37 °C. Subsequently, 3 mL aliquots were extracted from the dissolving medium at regular intervals of 1, 2, 4, 6, 12, and 24 h. Additionally, 3 mL of the same dissolution medium was replenished after each sampling event. The quantification of the absorbance of vemurafenib was performed at its maximum wavelength (λmax) of 307 nm. The concentration of vemurafenib that was presented in each sample was estimated using an equation derived from a calibration curve. The experiment was conducted three times, and the mean value was calculated. The cumulative quantity that was released was approximated as a percentage using the concentrations that were determined (26).

Preparation of ME-Based Hydrogel

The formulation that exhibited the highest level of refinement was selected as the basis for the hydrogel formulation (Table 2). Gelling agents were used to enhance the viscosity of the substances. One illustrative instance of such an agent is Carbomer 340, the hydrogel phase in the formulations was generated by dispersing Carbomer 940 in purified water using continuous stirring at a moderate speed with a mechanical shaker. Following this, the pH was adjusted to a desired range of 6 to 6.5 by using triethanolamine (TEA). Subsequently, the aforementioned combination was allowed to undergo a period of 24 h of rest, hence facilitating the thorough development and maturation of the hydrogel structure. The carbomer hydrogel was produced at concentrations of 1% and 2% w/v. Each ME that was chosen was then combined with the hydrogel in a 1:1 weight-to-weight ratio using a gentle stirring method. The ME-based hydrogel was obtained using a blending technique (27).

Table 2. The composition of different microemulsion-based hydrogel

	Carbomer 340		Formula			
Formula No.	1% W/V	2% W/V	BT1 (g)	BT2 (g)	OT1 (g)	OT2 (g)
GBT 1	4	-	4	-	-	-
GBT 2	-	4	4	-	-	-
GBT 3	4	-	-	4	-	-
GBT 4	-	4	-	4	-	-
GOT 1	4	-	-	-	4	-
GOT 2	-	4	-	-	4	-
GOT 3	4	-				4
GOT 4	-	4				4

Characterization of ME-Based Hydrogel

Visual appearance examination

These hydrogels were formulated as GBT1-GBT4 and GOT1-GOT4. Only the hydrogel exhibiting transparency and absence of phase separation was subjected to further experimentation (28).

pH measurement

The pH measurements were performed using a pH meter instrument (HANNA RI 02895, Romania). The calibration of the equipment was performed using standard buffer solutions with pH values of 7 and 4. After the calibration process, the probe of the device was submerged into each of the hydrogels formed with microemulsion, and the corresponding pH values were recorded (29).

Spreadability test

The evaluation of the spreadability of the hydrogel containing vemurafenib microemulsion was conducted by

measuring the weight of one gram from each sample and placing it at the central location of a designated circle on a glass slide. Following this, a supplementary glass slide was placed on top of the original one. Subsequently, an extra metallic weight with a mass of 2000 mg was placed on the upper glass slide for 3 min (29). The calculation of spreadability was determined by measuring the expansion of the border diameter of the hydrogel loaded with vemurafenib microemulsion as compared to its initial diameter used the equation (29).

$$\text{Spreadability} = \frac{\text{Weight placed (mg)} \times \text{Length of sample migration (cm)}}{\text{Time (sec)}}$$

Viscosity and Rheology study

A viscosity and rheology investigation were performed using a Brookfield digital viscometer (model NDJ–5S, manufactured in China). The No. 4 spindle of the device was introduced into each produced hydrogel based on microemulsion and thereafter revolved at different speeds (6, 12, 30, and 60 rpm) for 30 sec at each speed setting. The viscosity measurements were collected for each rotating speed (30).

Ex-vivo Permeability Study

Samples of 10 rat skin were obtained from male Swiss albino mice between the ages of 6 and 8 weeks. The process of removing abdominal hair from the sacrificed mice was conducted with great attention to detail using an electric shaver. A sample of skin, including the epidermis, stratum corneum, and dermis, was surgically removed from the shaved abdomen region. The dimensions of the excised slice were 2×2 cm. The precise excision of subcutaneous fat and connective tissues was thereafter performed utilizing operating scissors. The removal of blood from the tissue was performed in a gentle manner using soft paper. The examination of skin integrity was conducted with painstaking attention to detail using a microscope, and any areas of the skin that showed non-uniformity were excluded from the analysis. The skin samples were kept at a temperature of -20 °C and were used within one week after being obtained. To assess the skin penetration rate of various formulations of vemurafenib, excised mouse skin samples were affixed to Franz diffusion cells. Each sample was treated with 200 µg of hydrogel containing vemurafenib in a microemulsion-based formulation. The volume of the Franz diffusion cell was recorded as 12 mL, while the effective diffusion area was measured to be 1.76 cm^2. The receptor cell was filled with the FDA dissolving medium of vemurafenib, which consisted of 1% HTAB in a 0.05 M phosphate buffer solution at a pH of 6.8. The skin was placed on top of the receptor cell, with its outer layer facing the donor compartment. Subsequently, a ring with a hollow area of 1.76 cm^2 was placed onto the outermost layer of the skin, followed by the uniform distribution of 200 mg of hydrogel inside the ring. The Franz cell that had been produced was positioned within a temperature-controlled apparatus set at a temperature of 37°C, and it was rotated at a speed of 50 rpm. One milliliter of each samples were obtained at predetermined time intervals (1, 2, 4, 6, 12, 24 h) and then substituted with new receptor media (31). The absorbance of Vemurafenib at a wavelength of 307 nm was quantified, and the concentration of Vemurafenib in each sample was determined using an equation derived from a calibration curve. The cumulative release quantities were computed and standardized based on the area per unit.

Ex-vivo Skin Deposition Study

Following the skin permeability test, another test was carried out to assess skin retention. The skin samples were subjected to clean using a phosphate buffer solution with a pH of 7.4 to remove any remaining product residue. The skin samples that had been washed were divided into smaller sections, immersed in methanol for 24 h, and subjected to ultrasonicate for 30 min to remove the remaining vemurafenib. Following centrifugation at a speed of 6000 revolutions per minute for 10 min and subsequent removal of unwanted particles, the resulting liquid portion (supernatant) was subjected to filtrate using a membrane with a pore size of 0.45 µm. The absorbance of Vemurafenib, a specific compound of interest, was then determined using spectrophotometry at a wavelength of 305 nm. The quantification of skin deposition was performed using a relevant equation (31).

Skin Irritation Determination

Histological examination was employed to assess the skin irritation induced by the tested formulations. Sprague-Dawley rats were categorized into 3 groups, which included negative control group treated with pH 7.3 phosphate buffer, then remaining 2 groups were treated with selected formulations and their respective gel bases of GOT1 gel, and its Carbomer 340 gel base. Hair removal was meticulously carried out using an electric shaver one day before the skin irritation tests. During testing, 1mL of the test sample was uniformly applied to the shaved skin area of 3.46 cm^2 and then occluded with parafilm. Following a 24-hour exposure, the rats were sacrificed, and the applied skin tissue was excised for subsequent histological examination.

Statistical Analysis

The statistical analysis of all experimental data was conducted using IBM SPSS Statistics 25 software. The data were represented as the mean value accompanied by the standard deviation (SD). One-way Analysis of variance (ANOVA) was used, followed by a post hoc test (Tukey's HSD test), to establish the statistical significance of the observed differences. The predetermined threshold of significance was set at $P \leq 0.05$.

RESULTS AND DISCUSSION

Pseudo-ternary Phase Diagram

The results of this study showed the ternary phase diagram (Figure 1) visually represents the relationship between different ratios of TX-100, the presence of BMIM and OMIM ILs, and water. Figures 1A and 1B depict the ternary phase diagrams for the ionic liquids (ILs) BMIM and OMIM, respectively. In the provided diagrams, the shaded zone represents the domain where phase separation or macroemulsion formation occurs, while the unshaded or white region indicates the domain where single-phase microemulsion production takes place. The examination of the ternary phase diagram revealed a noticeable increase in the macroemulsion area as the length of the hydrocarbon chain in the ILs increased. Specifically, this shift occurred from 4 carbon atoms in the case of BMIM (Figure 1A) to 8 carbon atoms in the case of OMIM (Figure 1B). The results presented in this study are consistent with the existing knowledge that an increase in the hydrophobic nature of the ionic liquid results in a higher likelihood of observing macroemulsion or biphasic systems. Furthermore, the transition from a macroemulsion state to a microemulsion state requires a higher concentration of surfactants (32). In general, the impact of the hydrocarbon chain length of the ionic liquid on the ternary phase diagram is dependent upon the individual system under consideration, necessitating more research.

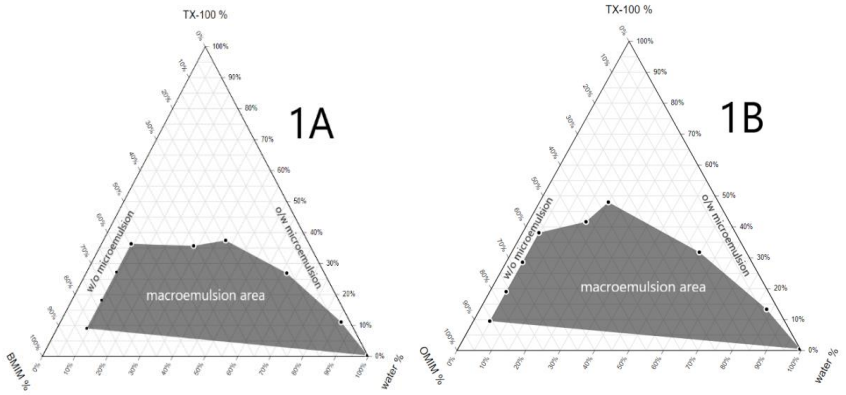

Figure 1. Pseudo ternary phase diagram. **(1A)** represent the pseudo ternary phase diagram when BMIM represents the oil phase, **(1B)** represent the pseudo ternary phase diagram when OMIM represents the oil phase

Percentage Transmittance and Refractive Index

The examination was conducted in Table 3 which demonstrated that both of the unladen ME and the ME, are containing vemurafenib that have transmittance levels above 98%. The measurement of light transmission percentage is a fundamental statistic used to evaluate the level of transparency shown by a given system. When the percentage transmittance (%T) reaches 100%, it indicates that the selected formulation exhibits high levels of clarity and transparency, as well as micelle sizes on the nanoscale scale (33).

Particle size, PDI of Vemurafenib MEs

Statistical analysis reveals no significant difference (P<0.05) between the formulas that share the same percentage of BMIM. namely, formula BT1 and BT2 display mean diameters ranging from 4.6±0.1 to 4.9±0.1 nm. The diameters exhibited consistency among microemulsions with different concentrations of BMIM. It is worth mentioning that the results obtained from dynamic light scattering (DLS) revealed a narrow distribution, which indicates the monodispersity of the microemulsion droplets. The finding that the size of microemulsion particles exhibited a notable rise as the percentage of BMIM escalated was particularly intriguing. This pattern was apparent in formulas BT1 and BT2, where the BMIM percentage was maintained at 10%, in addition to formula BT3, which increased the BMIM percentage to 15%. The hydrodynamic diameter (Dh) of the microemulsions exhibited a direct proportional relationship with the percentage of BMIM added, as anticipated. This finding suggests that the inclusion of BMIM caused the enlargement of the microemulsion particulates. This observation also suggests a roughly linear correlation between droplet radius and the percentage of BMIM (34). The aforementioned findings were replicated in formulations using OMIM as the oil phase during the production of IL/water ME. Furthermore, it was observed that the use of BMIM in the creation of ME resulted in a smaller droplet size compared to the use of OMIM when all the components were integrated in the ME formulation. The findings of this study align with the established concept that an increase in the hydrophobic nature of the ionic liquid is directly correlated with an expansion in the size of the droplets. The observed results have a strong resemblance to those often found in microemulsions consisting of ionic liquid-in-water (IL/W), hence providing more evidence for the hypothesis that IL/W microemulsions have been successfully generated (35).

Dilution test

All formulations, including ILs (either BMIM or OMIM) at a concentration of 10% w/w, were successfully passed the dilution test. These formulas, BT1, BT2, OT1, and OT2, demonstrated that the microemulsions were oil-in-water (o/w) as shown in Table 3. The formulae containing 15% w/w of ILs, namely BMIM or OMIM, were found to be unsuccessful in passing the dilution test. These formulations, namely BT3 and OT3, were unable to meet the requirements for being without ME (36).

Electrical conductivity test

The evaluation of conductivity (κ) in conventional water-in-oil (W/O) or oil-in-water (O/W) microemulsions provides valuable information on the percolative or anti-percolative properties shown by the system. It has been observed that in the context of conventional water-in-oil (W/O) systems, the conductivity stays negligible until a certain threshold of water percentage is reached, at which point it increases significantly by two to three orders of magnitude. Each of the created microemulsions, namely BT1-BT3 and OT1-OT3, demonstrated an electrical charge, indicating their classification as oil-in-water (o/w) microemulsions (37).

pH measurement of Vemurafenib Microemulsion

The pH values of the produced formulations (BT1-BT3 and OT1-OT3) fell within the range of 4.16±0.05 to 4.56±0.13, as shown in Table 3. These pH values are considered suitable for topical preparations. The pH of topical microemulsion exhibits variability based on the specific formulation and intended use. The stability, effectiveness, and propensity for skin irritation of a microemulsion may be influenced by its pH level. The pH of topical microemulsions may vary from 4 to 6 (38).

Drug Content

The drug concentration of all created formulations, namely BT1-BT3 and OT1-OT3, exhibited a range of 98.6±0.9% to 99.3±0.7%. The evaluation of dosage content homogeneity for topical transdermal preparations is mandated by the United States Pharmacopeia, which sets a maximum acceptability value of ±15%. This range is within an acceptable range for topical preparations, as indicated by reference (25).

In-vitro Drug Release

The drug release profile (Figure 2) of ME formulas that BMIM represented their oil phase was significantly (P<0.05) faster than that of corresponding ME formulas whose OMIM represented their oil phase. These observations can be explained by the high lipophilicity of OMIM that restricts the diffusion of the hydrophobic drug vemurafenib (vemurafenib has a high partition coefficient in OMIM). The release of the drug from ME primarily relies on a diffusion mechanism, where the drug moves from a lipid-rich liquid phase into an aqueous liquid phase. As a result, the sole remaining factor governing drug release is the partition coefficient (logD) between the lipophilic phase (IL) and the medium for release (39).

Table 3. Percentage transmittance particle size, polydispersity index (PDI), dilution test, electrical conductivity, pH, and drug content of vemurafenib microemulsion

Formula No.	Transmittance (%)	Particle size (nm)	*P*-value	PDI	*P*-value	Dilution test	Electrical Conductivity (µs/cm)	pH	Drug content (%)
BT1	98.1±0.20	4.90±0.10		0.21±0.02		Passed	1112±11	4.45±0.15	99.3±0.7
BT2	99.2±0.30	4.60±0.10	<0.001	0.16±0.01	0.012	Passed	253±10	4.43±0.01	98.6±0.8
BT3	98.4±0.10	11.2±1.00		0.18±0.01		Failed	219±5	4.28±0.04	98.8±0.5
OT1	99.3±0.50	7.9±0.10		0.17±0.02		Passed	316±5	4.34±0.05	98.6±0.9
OT2	99.5±0.70	7.1±0.20	<0.001	0.22±0.04	0.093	Passed	234±10	4.56±0.13	99.0±0.8
OT3	98.8±0.60	15±0.30		0.19±0.02		Passed	215±6	4.16±0.05	99.1±0.4

Results expressed as mean±SD

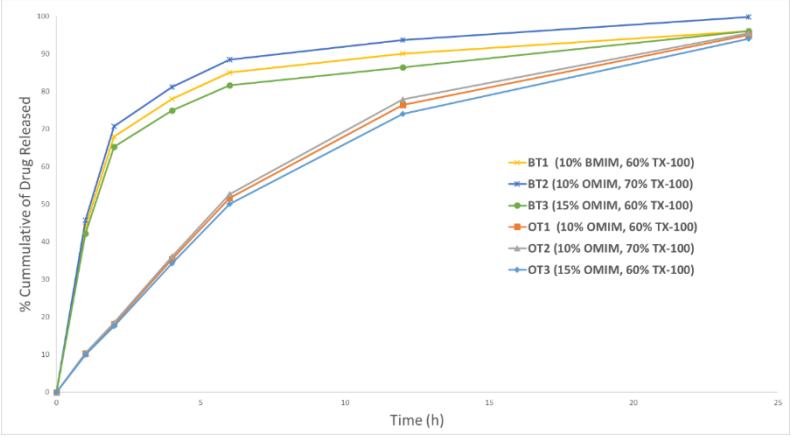

Figure 2. Release profile of vemurafenib from different microemulsion formulas (n=3). SE±Mean, statistical indices

Selection of MEs Formulation and Zeta Potential

Formulas BT1, BT2, OT1, and OT2 successfully underwent characterization tests for microemulsion and subsequently advanced to the stage of producing a hydrogel based on microemulsion. Formulas BT3 and OT3 exhibited failure during the dilution test, thereby rendering them unsuitable for inclusion in the formulation of the microemulsion-based hydrogel. The zeta potential values for formulae BT1, BT2, OT1, and OT2 were determined to be -0.42± 0.08, -0.54±0.06, -0.45±0.04, and -0.65±0.07, respectively. The low zeta-potential values of the prepared microemulsion may be attributed to the low salinity and ionic strength of the prepared microemulsion (40). However, there is no risk of particle aggregation since the prepared microemulsion would be incorporated into a gel base that would reserve the separation between microemulsion particulates.

Characterization of MEs-Based Hydrogel

Visual appearance

As a result of these results, only the hydrogels containing OMIM (GOT1-GOT4) were selected for further evaluation in the hydrogel characterization tests. Upon analyzing the hydrogels that were synthesized, it was seen that the hydrogels containing BMIM (designated as formulae GBT1-GTB4) had a visually perceptible creamy white color. Furthermore, these hydrogels underwent phase separation, resulting in the formation of a two-layered system over a period of time. On the other hand, hydrogels synthesized with OMIM (formulas GOT1-GOT4) exhibited a lack of color and demonstrated transparency without any observable indications of phase separation. The reason could be attributed to the higher charge of the more hydrophilic BMIM compared to more OMIM which caused a breakdown of the gel structure of the Carbamer 340 gel base (41).

pH and Spreadability

The pH values (Table 4) were observed in this study fell within a range of 5.33±0.11 to 5.84±0.42, which is consistent with the permissible guidelines established for topical formulations. Consequently, these pH levels do not pose any discernible risk of skin irritation. Significantly, discrepancies in the spreadability of the hydrogels that were synthesized were noticed, which might likely be attributed to differences in their relative viscosities (42, 43).

Viscosity and Rheology of hydrogel

The microemulsion-based hydrogel formulations (GOT1-GOT4) exhibited rheological properties that followed a non-Newtonian shear-thinning pattern. This behavior was seen as a reduction in viscosity with increasing shear rates, as shown in Figure 3. Under the influence of increased shear stress, the molecular structure of the gelling agent underwent reorientation, causing the disordered molecules to align their long axes in the direction of the flow. The process of realignment caused a drop in internal resistance inside the material, resulting in a corresponding reduction in viscosity. The researchers hypothesized that there would be a positive correlation between the concentration of Carbomer 340 (1-2%) and the viscosity, as seen in Table 4. These observations may be explained by the enhanced crosslinking effect resulting from the higher polymer content (42).

Table 4. pH, spreadability, and viscosity at 6 rpm of different microemulsion-based hydrogels. SE±Mean, n= statistical indices also abbreviation

Formula No.	pH	*P*-value	Spreadability (g.cm/sec)	*P*-value	Viscosity (mPa.s) at 6 rpm	*P*-value
GOT1	5.33±0.11	0.2167	80.4±0.1	0.100	42221±655	0.028
GOT2	5.84±0.42		81.7±0.4		84443±131	
GOT3	5.63±0.08		80.0±0.5		33569±344	
GOT4	5.40±0.06		81.7±0.5		54723±380	

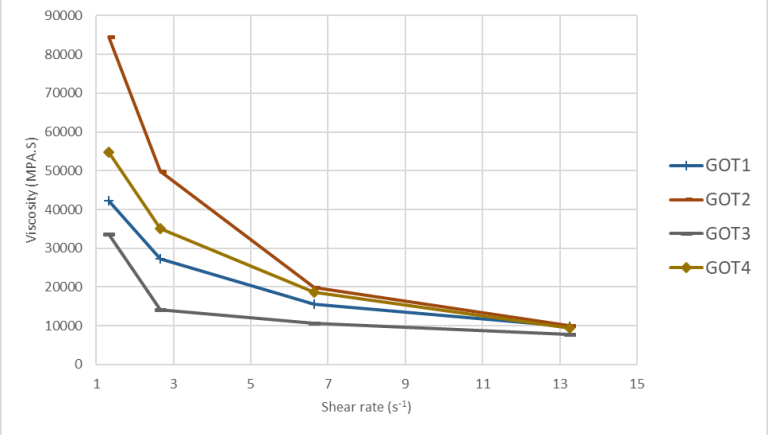

Figure 3. The rheological behavior of different microemulsion-based hydrogel formulas. SE±Mean, n= statistical indices

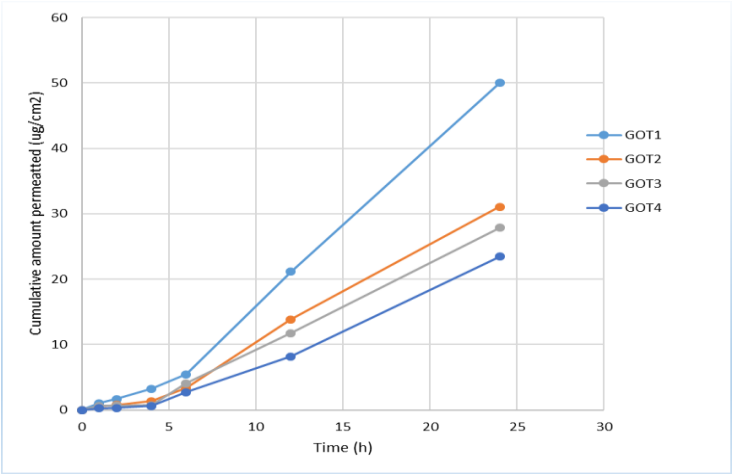

Figure 4. Accumulation of permeated substance per square centimeter over time across various hydrogel formulations based on microemulsions. SE±Mean, n= statistical indices

Table 5. represents Jss, T_{lag}, K_p, vem permeated in 24 h (%) and Skin deposition (µg) of different microemulsion based hydrogel of different microemulsions based hydrogel

Formula No.	Jss (µg/cm².h)	*P*-value	T_{lag} (h)	*P*-value	K_p (cm/h)	vem permeated in 24 h (%)	*P*-value	Skin deposition (%)	*P*-value
GOT1	2.4638	<0.001	8.9573	<0.001	0.002464	44.2	0.020	40.8±0.5	0.005
GOT2	1.5244		5.2689		0.001524	27.4		25.6±0.7	
GOT3	1.3237		3.939		0.001324	24.0		19.8±0.4	
GOT4	1.1707		4.9379		0.001171	20.7		16.8±0.2	

Ex-vivo permeability study and skin deposition

Figure 4 illustrated the cumulative permeation per square centimeter over time for several hydrogel formulations derived from microemulsions, denoted as GOT1-GOT4. In a comparative investigation of the permeability coefficients (Kp) and flux (Jss) of vemurafenib, as shown in Table 5, the hydrogels GOT1 and GOT2 were examined. These hydrogels were generated from the identical microemulsion OT1. The results indicate that GOT1 demonstrated considerably higher values (P<0.05) for both Jss and Kp compared to GOT2. The observed difference in viscosity between the GOT1 hydrogel (measuring 42221±655 mP.s at 6 rpm) and the GOT2 hydrogel (measuring 84443±131 mP.s at 6 rpm) might be attributed to the lower viscosity of the former. It is worth mentioning that the increased viscosity observed in the hydrogel matrix seemed to hinder the release of vemurafenib. This finding establishes a negative correlation between hydrogel viscosity and the rate of vemurafenib release, which aligns with the notion that higher viscosity impedes drug release (44). A similar pattern is seen when examining the permeability profiles of GOT3 and GOT4 hydrogels, derived from the microemulsion OT2. Specifically, GOT3 exhibits a permeability measurement of 33569±344 mP.s at 6 rpm, whereas GOT4 demonstrates a permeability measurement of 54723±380 mP.s at 6 rpm. The potential mechanisms that could explain the enhancement of the microemulsion system can be attributed to the following factors: Firstly, the surfactant components may act as permeation enhancers. Secondly, the small droplet size at the nanoscale may facilitate greater hydration of the skin layer. Lastly, the observed decrease in viscosity could contribute to increased permeability (42).

In addition, the incorporation of OMIM: TX-100 in the microemulsion utilized in the synthesis of various hydrogels affected the steady-state flow (Jss) and permeability coefficient (Kp) values. It was noted that hydrogel formulations comprising a greater proportion of OMIM to TX-100 exhibited higher values of Jss and Kp in comparison to the other hydrogels that were produced. It was observed that formula GOT1, with an OMIM: TX-100 ratio of 1:6 w/w, demonstrated significantly higher values of Jss and Kp ($\boldsymbol{U}$ < 0.05) in comparison to formula GOT2, which possessed the same ratio at 1:7 w/w. This performance disparity was noted notwithstanding the fact that GOT1 had a significantly higher viscosity than GOT2. An analogous trend was observed upon scrutinizing the Jss and Kp values in relation to GOT3 and GOT4, as illustrated in Table 5. This phenomenon can be elucidated by considering the characteristic of ionic liquids (ILs) to possess hydrophilic or lipophilic groups that augment permeability. The hydrophilic component of ionic liquids (ILs) has been seen to disturb the tight junctions inside the stratum corneum (SC), hence enabling paracellular transport and encouraging fluidization within the protein and lipid domains. On the other hand, lipophilic ionic

liquids (ILs) have been seen to increase the partitioning process inside the epithelium by forming channels that aid in transcellular transport across the lipid regions (45-53). Skin deposition studies were performed to evaluate the potential of the hydrogel formulation containing vemurafenib for the treatment of melanoma by topical application. Significantly, the hydrogel known as GOT1 had the highest level of skin deposition, with a recorded deposition rate of 40.8±0.5% (54, 55).

Skin Irritation

The irritation test was carried out to evaluate the safety of the tested microemulsion-based formulations, utilizing phosphate buffer-treated skin as the negative control showed normal tissue structure. While treated groups showed that the skin tissue exhibited completeness and well-defined characteristics. In the tested drug-free gels (Carbamer 340 gel) and microemulsion-loaded gel formulations (GOT1), no apparent erythema and edema were observed when compared to the negative group (except for small edema and some mild inflammation in the control negative group that may attributed to small injuries during preparing the animal to the tests). This indicates that the designed microemulsion-based gel formulation demonstrates good biocompatibility with skin tissue.

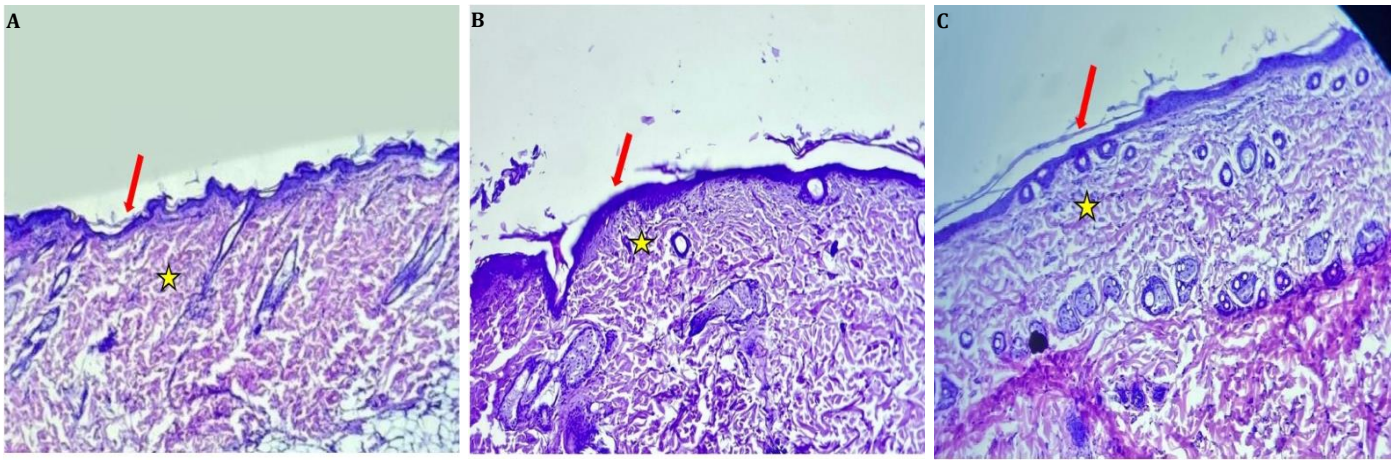

Figure 5. Photographic images for rate shin histology treated with **(A)** phosphate buffer 7.4 and showed a normal epidermis (Red arrow) and dermal fibrous tissue (star), **(B)** Carbamer 340 gel showed a normal epidermis (Red arrow) and dermal fibrous tissue (star), and **(C)** GOT 1 gel and showed a normal epidermis (Red arrow) and dermal fibrous tissue (star)

This may indicate that the designed microemulsion-based gel formulation demonstrates good biocompatibility with skin tissue. Topical delivery of vemurafenib is a promising route of drug administration to melanoma skin. Ionic liquids (ILs) have permeation-enhancing properties with either hydrophilic or lipophilic characteristics.

Acknowledgements

N/A

Conflict of Interest

The authors declare no conflict of interest.

References

1. Schadendorf D, van Akkooi ACJ, Berking C, Griewank KG, Gutzmer R, Hauschild A, et al. Melanoma. The Lancet. 2018;392(10151):971-984. 10.1016/S0140-6736(18)31559-9
2. Larkin J, Ascierto PA, Dréno B, Atkinson V, Liszkay G, Maio M, et al. Combined vemurafenib and cobimetinib in BRAF-mutated melanoma. N Engl J Med. 2014;371(20):1867-1876. 10.1056/NEJMoa1408868
3. Chapman PB, Robert C, Larkin J, Haanen JB, Ribas A, Hogg D, et al. Vemurafenib in patients with BRAFV600 mutation-positive metastatic melanoma: final overall survival results of the randomized BRIM-3 study. Ann. Oncol. 2017;28(10):2581-2587. 10.1093/annonc/mdx339
4. Spengler EK, Kleiner DE, Fontana RJ. Vemurafenib-induced granulomatous hepatitis. Hepatology. 2017;65(2):745-748.
5. Almajidi YQ, Maraie NK, Raauf AMR. Utilization of solid in oil nanodispersion to prepare a topical vemurafenib as potential delivery system for skin melanoma. Appl Nanosci. 2023;13(4):2845-2856. 10.1007/s13204-021-02158-y
6. Szumała P, Macierzanka A. Topical delivery of pharmaceutical and cosmetic macromolecules using microemulsion systems. Int. J. Pharm. 2022;615:121488. 10.1016/j.ijpharm.2022.121488
7. Al-Rubaye RA, Al-Kinani KK. Formulation and evaluation of prednisolone acetate microemulsion ocular gel. Egy J Hosp Med. 2023;90(1):1744-1751. 10.21608/ejhm.2023.284303
8. Somasundaran P, editors. Encyclopedia of surface and colloid science, 2nd edition; CRC Pr I Llc;United states. 2006. 2372 p.
9. Prat D, Hayler J, Wells A. A survey of solvent selection guides. Green Chem. 2014;16(10):4546-4551. 10.1039/C4GC01149J
10. Blacklock KL, van der Weyden L. Advances in understanding spontaneously occurring melanoma in animals. Vet. Sci. 2023;10(3):210. 10.3390/vetsci10030210
11. Battaglia L, Scomparin A, Dianzani C, Milla P, Muntoni E, Arpicco S, et al. Nanotechnology addressing cutaneous melanoma: The Italian landscape. Pharmaceutics. 2021;13(10):1617. 10.3390/pharmaceutics13101617
12. Ha L, Noonan FP, De Fabo EC, Merlino G. Animal models of melanoma. J Investig Dermatol Symp Proc. 2005;10:86-88. 10.1111/j.1087-0024.2005.200409.x
13. Farooq SU, Kumar DS, Shahid AA. Formulation and Evaluation of Vitamin D3 (Cholecalciferol) Self-Nanoemulsifying Drug Delivery

Systems for Enhancing Solubility. Int J Pharm Biol Sci. 20199(3):587-598. 10.21276/ijpbs.2019.9.3.76
14. Hamed SB, Abd Alhammid SN. Formulation and characterization of felodipine as an oral nanoemulsions. Iraqi J. Pharm. Sci. 2021;30(1):209-217. 10.31351/vol30iss1pp209-217
15. Naeem M. Microemulsion and microemulsion based gel of Zaleplon for transdermal delivery: Preparation, optimization, and evaluation. Acta Pol Phar-Drug Res. 2019;76(3):543-561. 10.32383/appdr/10166
16. Hajjar B, Zier K-I, Khalid N, Azarmi S, Löbenberg R. Evaluation of a microemulsion-based gel formulation for topical drug delivery of diclofenac sodium. J Pharm Investig. 2018;48:351-362. 10.1007/s40005-017-0327-7
17. Tiwari N, Sivakumar A, Mukherjee A, Chandrasekaran N. Enhanced antifungal activity of Ketoconazole using rose oil based novel microemulsion formulation. J Drug Deliv Sci Technol. 2018;47:434-444. 10.1016/j.jddst.2018.07.007
18. Hammodi ID, Abd Alhammid SN. Preparation and characterization of topical letrozole nanoemulsion for breast cancer. Iraqi J. Pharm. Sci. 2020;29(1):195-206. 10.31351/vol29iss1pp195-206
19. Basheer HS, Noordin MI, Ghareeb MM. Characterization of microemulsions prepared using isopropyl palmitate with various surfactants and cosurfactants. Trop J Pharm Res. 2013;12(3):305-310. 10.4314/tjpr.v12i3.5
20. Thakkar H, Nangesh J, Parmar M, Patel D. Formulation and characterization of lipid-based drug delivery system of raloxifene-microemulsion and self-microemulsifying drug delivery system. J. Pharm Bioallied Sci. 2011;3(3):442. 10.4103/0975-7406.84463
21. Yadav V, Jadhav P, Kanase K, Bodhe A, Dombe S. Preparation and evaluation of microemulsion containing antihypertensive drug. Int J Appl Pharm. 2018;10(5):138-146. 10.22159/ijap.2018v10i5.27415
22. Iradhati AH, Jufri M. Formulation and physical stability test of griseofulvin microemulsion gel. Int J Appl Pharm. 2017;9:23-26. 10.22159/ijap.2017.v9s1.22_27
23. Ghareeb MM. Formulation and characterization of isradipine as oral nanoemulsion. Iraqi J Pharm Sci. 2020;29(1):143-153. 10.31351/vol29iss1pp143-153
24. Liu D, Lu H, Zhang Y, Zhu P, Huang Z. Conversion of a surfactant-based microemulsion to a surfactant-free microemulsion by CO_2. Soft Matter. 2019;15(3):462-469. 10.1039/C8SM02444H
25. Ali FR, Shoaib MH, Yousuf RI, Ali SA, Imtiaz MS, Bashir L, et al. Design, development, and optimization of dexibuprofen microemulsion based transdermal reservoir patches for controlled drug delivery. Biomed Res. Int. 2017;17(1):1-15. 10.1155/2017/4654958
26. Dawood NM, Abdul-Hammid SN, Hussein AA. Formulation and characterization of lafutidine nanosuspension for oral drug delivery system. Int J Appl Pharm. 2018;10(2):20-30. 10.22159/ijap.2018v10i2.23075
27. Khullar R, Kumar D, Seth N, Saini S. Formulation and evaluation of mefenamic acid emulgel for topical delivery. Saudi Pharm J. 2012;20(1):63-67. h10.1016/j.jsps.2011.08.001
28. Pranali S, Charushila S, Sayali C, Namrata M. Design and characterisation of emulgel of an antifungal drug. J. Pharm. Res. 2019;11(6):2357-2361.
29. Jaber SA, Sulaiman HT, Rajab NA. Preparation, characterization and *in-vitro* diffusion study of different topical flurbiprofen semisolids. IJDDT. 2020;10(1):81-87. 10.25258/ijddt.10.1.12
30. Sabri LA, Sulayman HT, Khalil YI. An investigation release and rheological properties of miconazole nitrate from Emulgel. Iraqi J Pharm Sci. 2009;18(2):26-31.
31. Tung N-T, Vu V-D, Nguyen P-L. DoE-based development, physicochemical characterization, and pharmacological evaluation of a topical hydrogel containing betamethasone dipropionate microemulsion. Colloids and Surfaces B: Biointerfaces. 2019;181:480-488. 10.1016/j.colsurfb.2019.06.002
32. Swatloski RP, Visser AE, Reichert WM, Broker GA, Farina LM, Holbrey JD, et al. On the solubilization of water with ethanol in hydrophobic hexafluorophosphate ionic liquids. Green Chem. 2002;4(2):81-87. 10.1039/B108905F
33. Smail SS, Ghareeb MM, Omer HK, Al-Kinani AA, Alany RG. Studies on surfactants, cosurfactants, and oils for prospective use in formulation of ketorolac tromethamine ophthalmic nanoemulsions. Pharmaceutics. 2021;13(4):467. 10.3390/pharmaceutics13040467
34. Zheng Y, Eli W. Study on the polarity of bmimPF6/Tween80/toluene microemulsion characterized by UV-visible spectroscopy. J Dispersion Sci Technol. 2009;30(5):698-703. 10.1080/01932690802553890
35. Safavi A, Maleki N, Farjami F. Phase behavior and characterization of ionic liquids based microemulsions. Colloids and Surfaces A: Physicochem Eng Aspects. 2010;355(1-3):61-66.
36. Ryu K-A, Park PJ, Kim S-B, Bin B-H, Jang D-J, Kim ST. Topical delivery of coenzyme Q10-loaded microemulsion for skin regeneration. Pharmaceutics. 2020;12(4):332.
37. Łuczak J, Hupka J. Studies on formation and percolation in ionic liquids/TX-100/water microemulsions. J Mol Liq. 2014;199:552-558.
38. Murthy SN, Shivakumar HN. Topical and transdermal drug delivery. Handbook of non-invasive drug delivery systems: William Andrew, New York, US; 2010. p. 1-36. 10.1080/01932690802553890
39. Bernkop-Schnürch A, Jalil A. Do drug release studies from SEDDS make any sense? J Control Release. 2018;271:55-59. 10.1016/j.jconrel.2017.12.027
40. Pal N, Kumar S, Bera A, Mandal A. Phase behaviour and characterization of microemulsion stabilized by a novel synthesized surfactant: Implications for enhanced oil recovery. Fuel. 2019;235:995-1009. 10.1016/j.fuel.2018.08.100
41. Joshi SC. Sol-gel behavior of hydroxypropyl methylcellulose (HPMC) in ionic media including drug release. Materials. 2011;4(10):1861-905. 10.3390/ma4101861
42. ALEXANDER I, KRASNYUK II. Dermatologic gels spreadability measuring methods comparative study. Int J Appl Pharm. 2022;14(1):164-168. 10.22159/ijap.2022v14i1.41267
43. Nikumbh KV, Sevankar SG, Patil MP. Formulation development, in vitro and in vivo evaluation of microemulsion-based gel loaded with ketoprofen. Drug Deliv. 2015;22(4):509-515. 10.3109/10717544.2013.859186
44. Vu QL, Fang C-W, Suhail M, Wu P-C. Enhancement of the topical bioavailability and skin whitening effect of genistein by using microemulsions as drug delivery carriers. Pharmaceuticals. 2021;14(12):1233. 10.3390/ph14121233
45. Abdul-Aziz BI, Rajab NA. Preparation and in-vitro evaluation of mucoadhesive clotrimazole vaginal hydrogel. Iraqi J Pharm Sci. 2014;23:1-7.
46. Navti PD, Pandey A, Nikam AN, Padya BS, Kalthur G, Koteshwara KB, et al. Ionic liquids assisted topical drug delivery for permeation enhancement: Formulation strategies, biomedical applications, and toxicological perspective. AAPS PharmSciTech. 2022;23(5):161. 10.1208/s12249-022-02313-w
47. Agatemor C, Ibsen KN, Tanner EEL, Mitragotri S. Ionic liquids for addressing unmet needs in healthcare. Bioeng. Transl Med. 2018;3(1):7-25. 10.1002/btm2.10083
48. Zhang Y, Liu C, Wang J, Ren S, Song Y, Quan P, et al. Ionic liquids in transdermal drug delivery system: Current applications and future perspectives. Chinses Chem Lett. 2023;34(3):107631. 10.1016/j.cclet.2022.06.054
49. Sadaf A, Sinha R, Ekka MK. Ionic liquid-mediated skin technologies: Recent advances and prospects. Curr. Res. Biotechnol. 2022. 10.1016/j.crbiot.2022.10.005
50. Beaven E, Kumar R, Ahn JM, Mendoza H, Sutradhar SC, Choi W, et al. Potential of Ionic liquids to overcome physical and biological barriers to enable oral and topical administration. Adv. Drug Deliv. Rev. 2023:115157. 10.1016/j.addr.2023.115157
51. Yu Y-Q, Yang X, Wu X-F, Fan Y-B. Enhancing permeation of drug molecules across the skin via delivery in nanocarriers: novel strategies for effective transdermal applications. Front. bioeng. biotechnol. 2021;9:646554. 10.3389/fbioe.2021.646554
52. Phatale V, Vaiphei KK, Jha S, Patil D, Agrawal M, Alexander A. Overcoming skin barriers through advanced transdermal drug

delivery approaches. J Control Release. 2022;351:361-80. 10.1016/j.jconrel.2022.09.025
53. Anselmo AC, Gokarn Y, Mitragotri S. Non-invasive delivery strategies for biologics. Nat Rev Drug Discov. 2019;18(1):19-40. 10.1038/nrd.2018.183
54. Agatemor C, Ibsen KN, Tanner EE, Mitragotri S. Ionic liquids for addressing unmet needs in healthcare. Bioeng. Transl Med. 2018;3(1):7–25. 10.1002/btm2.10083
55. Lim GS, Jaenicke S, Klähn M. How the spontaneous insertion of amphiphilic imidazolium-based cations changes biological membranes: A molecular simulation study. Phys Chem Chem Phys. 2015;17(43):29171–29183. 10.1039/C5CP04806K

توصيف ودراسة تهيج جلد الحيوان للهيدروجيل المستند إلى مستحلب دقيق فيمورافينيب باستخدام السائل الأيوني كطبقة زيتية

محمد جاسم نعمة، انتظار جاسم العكام

فرع الصيدلانيات، كلية الصيدلة، جامعة بغداد، بغداد، العراق

الخلاصة

يمثل سرطان الجلد الجلدي معدل وفيات سنوي يبلغ ٥٥٥٠٠ شخص. تم ترخيص استخدام مثبطات الكيناز ذات الجزيئات الصغيرة عن طريق الفم، والتي تستهدف على وجه التحديد BRAFv600، كاستراتيجية علاجية رئيسية للحالات المتقدمة والمنتشرة ارتبط تناول vemurafenib عن طريق الفم، وهو مثبط BRAFv600، بحدوث تأثيرات ضارة في حوالي ٣٠٪ من الأفراد الذين يخضعون للعلاج. يهدف هذا البحث إلى تطوير استراتيجية العلاج الموضعي للدواء باستخدام المستحلبات الدقيقة لتعزيز توزيعه عبر الجلد. تم إنتاج المستحلبات الدقيقة من خلال إذابة vemurafenib في مزيج من السائل الأيوني (١-بوتيل-٣-ميثيلميدازوليوم سداسي فلوروفوسفات أو ١-أوكتيل-٣-ميثيليميدازوليوم سداسي فلوروفوسفات) والعامل الفاعل بالسطح (Triton x-100). تم إجراء سلسلة من التقييمات لتقييم الاستقرار الجسدي، وتحديد الرقم الهيدروجيني، وفحص تجانس المحتوى، وتحليل إطلاق الدواء في المختبر. اجتازت أربع صيغ من مستحلبات Vemurafenib الدقيقة جميع اختبارات توصيف وتقييم المستحلبات الدقيقة. كانت أقطار القطرات في هذه المستحلبات الدقيقة ضمن نطاق المستحلبات الدقيقة (أقل من ٢٠٠ نانومتر). ثم تم استخدامها لإنشاء الهلاميات المائية القائمة على المستحلبات الدقيقة، باستخدام Carbamer 340 كعامل تبلور عن طريق إجراء طريقة خلط بسيطة. فقط الهلاميات المائية المتكونة من المستحلبات الدقيقة التي تحتوي على ١-أوكتيل-٣-ميثيلميدازوليوم سداسي فلوروفوسفات أظهرت القدرة على تكوين الهلاميات المائية الواضحة ذات الاتساق المرغوب فيه. فيما يتعلق بدراسة النفاذية خارج الجسم الحي وترسب الجلد، تُظهر ملفات تعريف النفاذية الخاصة بصيغة GOT3 قياس نفاذية يبلغ ٣٣٥٦٩ ± ٣٤٤ ميلي بيكسل في الثانية عند ٦ دورة في الدقيقة، في حين يُظهر GOT4 قياس نفاذية قدره ٥٤٧٢٣ ± ٣٨٠ ميلي بيكسل في الثانية عند ٦ دورة في الدقيقة. أثناء اختبار تهيج الجلد، لم يلاحظ أي وذمة واضحة. يشير هذا إلى أن تركيبة الجل المصممة القائمة على المستحلبات الدقيقة توضح توافقًا حيويًا جيدًا مع أنسجة الجلد. يعد التسليم الموضعي لـ vemurafenib طريقًا واعدًا لإيصال الدواء لعلاج سرطان الجلد. كما وتتمتع السوائل الأيونية (ILs) بخصائص معززة للنفاذ مع خصائص محبة للماء أو محبة للدهون.

الكلمات المفاحية: المستحلب الدقيق، السائل الأيوني